Vol. 04, Iss. 1 (2026) 88-94, DOI: 10.61552/JME.2026.01.009

JME

Journal of Materials and Engineering

www.jme.aspur.rs

Research article

Solid Particle Erosion on a Tepetate-Based Ceramic Material

Juan Rodrigo Laguna Camacho[a,*], Raúl Enrique Contreras-Bermúdez[b], Ezequiel Alberto Gallardo-Hernández[c], Alejandra Velasco-Pérez[d], Manuel Vite-Torres[c], Heriberto Esteban-Benito[e]

[a]*Universidad Veracruzana, Faculty of Mechanical and Electrical Engineering, Poza Rica, Veracruz, Mexico,*
[b]*Universidad Veracruzana, Faculty of Chemical Sciences, Poza Rica, Veracruz, Mexico,*
[c]*Tribology Group, Department of Mechanical Engineering, Instituto Politécnico Nacional, SEPI-ESIME-U. Zacatenco, Mexico City, Mexico,*
[d]*Universidad Veracruzana, Faculty of Chemical Sciences, Orizaba, Veracruz, Mexico,*
[d]*Tecnológico Nacional de México/Instituto Tecnológico Superior de Naranjos, Naranjos, Veracruz, Mexico.*

Keywords:

Solid particle erosion
Tepetate-based ceramic material
Alumina particles
ASTM G76

* Corresponding author:

Juan Rodrigo Laguna Camacho
E-mail: jlaguna@uv.mx

Received: 2 October 2025
Revised: 1 November 2025
Accepted: 2 December 2025

A B S T R A C T

In this research work, solid particle erosion tests were carried out to evaluate the performance of a new tepetate-based ceramic material. The novelty of this work is the use of tepetate (yellow earth) from Mexico, as a base for making bricks that could be used for construction applications. The tepetate is mixed with specific portions of sand and water to obtain the bricks. Once the bricks were obtained with specific measurements, erosion tests were performed according to ASTM G76 standard. The samples of the ceramic material were subjected to the impact of alumina particles at different impact angles, 30°, 45°, 60° and 90° to evaluate their erosion resistance. In these particular tests, the particle velocity was very low, 5 ± 1 m/s, to prevent the samples from breaking into pieces. In addition, the morphology of the alumina particles was determined using SEM and their chemical composition was acquired by EDS analysis. Finally, the mass loss and erosion rates were obtained and the results are presented in this paper.

1. INTRODUCTION

Tepetate is a granular material derived from a clay found in thick, massive open-air layers. It is lightweight and has a yellowish color. Because tepetate is porous, it is excellent for absorbing water. It also serves as an insulator, which is why it is used to make bricks in many cities with extreme climates. Tepetate extraction is simple and can be done with a pick and shovel, as it is a very lightweight material. This makes it ideal for use as fill between floors. Due to its light weight, tepetate often replaces tezontle (porous volcanic stone). Tepetate is also used in bathroom fill, as

fine aggregate, and, as previously mentioned, tepetate is used for the construction of ashlars for walls (it is recommended to alternate it with red brick for greater strength) [1]. In relation to the erosion damage due to the impact of solid particles, this significant wear process has been reported as a major problem in different mechanical elements such as gas turbine blades, military aircraft, tillage tools, ceramic pipes, wind turbines and helicopter rotor blades [2]. Several studies have been conducted on erosion of different ceramic materials, for instance on ceramic matrix composites [3], zirconia ceramics [4], laminated ceramic structures [5], and alumina and silicon nitride ceramics [6] at diverse testing conditions as particle velocities, flow rates, impact angles, abrasive particles (hardness, shapes and sizes) and low and high temperatures [7]. The results have shown that some ceramic materials present a ductile behaviour reaching their maximum erosion rates at low incident angles ($\alpha \leq 45°$) whereas other exhibit a brittle performance with greater erosion rates at high impact angles ($\alpha > 45°$), especially at normal incidence (90°) [8].

Due to the importance of ceramic materials in different types of industries, this work describes the methodology used to manufacture the samples (bricks) of novel tepetate-based ceramic that were subjected to erosion tests, under very specific conditions. In addition, the erosion rate results and an explanation of the material behavior (ductile or brittle) are presented. This work is a continuation of the research being conducted on different ceramic materials.

2. EXPERIMENTAL PROCEDURE

2.1 Fabrication of ceramic material samples made from tepetate

The material used for the erosion tests was a tepetate-based ceramic. This material presented a porous structure, making its characterization interesting. The tested samples had the following approximate dimensions: 50 mm x 25 mm x 6 mm thickness (small bricks) and are shown in Figure 1. In relation to the production of the bricks that were used as specimens to perform the solid particle erosion tests, these were made with tepetate (yellow earth) that originates in Mexico and also sand, these materials were extracted from hills (benches) located in the region known as "El Chote" in the city of Poza Rica, in the state of Veracruz (Figure 2) [9]. The brick manufacturing process is as follows: first, a mixture is prepared with tepetate (yellow earth) (50% Wt.) and sand (50% Wt.); and certain portions of water are permanently added, until the appropriate or required consistency is obtained (solid mixture). Next, this mixture (tepetate + sand + water) is poured with shovels into a mill, whose shape is a square container with an outlet at the bottom rear, which is where the plastic mass is emitted, before carrying out the kneading process. In respect to the kneading process, an earth rammer is used to obtain the plastic mass that will later be moulded. The required consistency is determined by touch, that is, empirically and based on the knowledge of the worker in charge of the kneading. Subsequently, the brick moulding process consists of depositing a certain amount of the mixture (tepetate + sand + water) to fill the mould cavity, as shown in Figure 3. Once the moulds are full, the excess material is removed with a metal or wooden ruler, known as a "scraper." This is done to give the bricks a smooth finish. The wastes removed with the scraper are returned to the mix pile for reuse. The mix is then emptied from the moulds onto a designated surface, usually exposed to light. This ensures the paste is moulded and ready to dry. This process must be repeated as many times as necessary until the entire mix is moulded. It should be noted that the resulting product is known as green brick. Immediately after the bricks have been moulded, the pre-drying stage begins. The pre-formed paste should be left for approximately 4 hours, or until it can be handled. Green bricks can even be covered with tarps or plastic bags to prevent cracking from sunlight. When the pre-formed paste is dry enough to be handled, it is rotated 90° so that the surface facing the ground can shed any moisture it contained. If necessary, the burrs are removed from the brick with a smooth wooden shaving brush, which also helps to give it a better finish. This activity is known as edging (Figure 4). Drying is completed until the raw brick loses approximately 13% moisture. The bricks should remain for approximately 1 to 2 weeks, depending on the climate in the region. The brick kiln is loaded (artisanal) when the preformed or moulded bricks are completely dry. When the bricks are being introduced into the kiln, they must be placed on plates called tables. These tables must be arranged in a special way to achieve the correct distribution of the heat generated by the burner flame. Finally, the firing process consists of firing the previously

dried bricks loaded into the kiln with the help of a fuel. The most common fuels are fuel oil, firewood, coal, diesel, and burned engine oil. This process ensures that the bricks acquire their mechanical and physical properties (strength and colour), since unfired clay has very low properties, as well as their final appearance (Figure 4). This operation takes approximately 24 hours, so the fuel and water supply is continuous throughout the firing process. The fuel commonly used is recycled oil, with approximately 7,000 litters used for the firing process of 40,000 bricks.

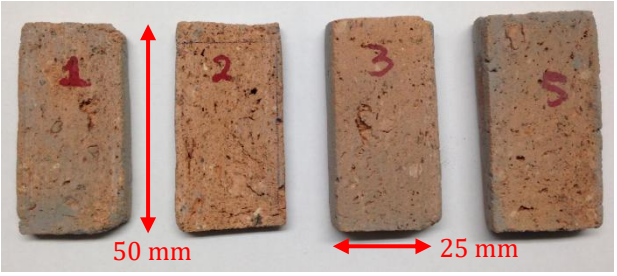

Fig. 1. Samples of tepetate-based ceramics before erosion tests.

Fig. 2. Extraction hills (benches).

(a)

(b)

Fig. 3a-b. Brick molding process.

(a)

(b)

Fig. 4a-b. Drying the bricks.

2.2 Characterization of ceramic material

The ceramic brick made from tepetate was characterized by X-ray diffraction (XRD) (Panalytical diffractometer model XPERT MRD). To do this, small segments of

approximately 1 cm^2 were cut from samples. The X-ray diffraction results were obtained using CuKα radiation to identify the chemical phases that make up the brick. Figure 5 shows the diffraction pattern of the brick with no damage before the erosion tests. Among the phases that were identified, it is possible to observe copper-zirconium phosphate ($CuZr_2(PO_4)_3$), silicon oxide (SiO_2) and calcite ($CCa_{0.936}Mg_{0.064}$).

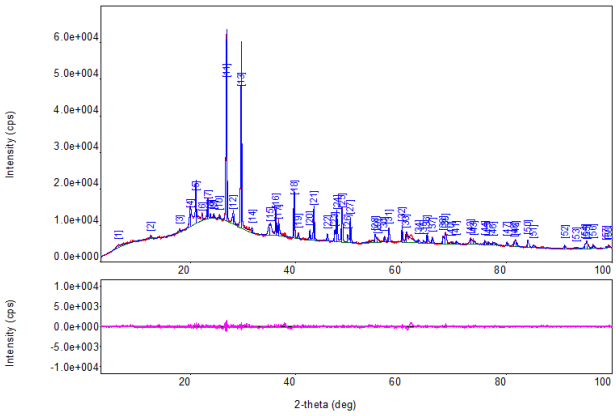

Fig. 5. DRX brick pattern made from tepetate.

2.3 Characterization of aluminium oxide

In respect to the characterization of aluminium oxide, the first step was to perform the analysis of the particle size distribution by using the equipment Analysette 28 Image Analyzer (Fritsch), which is an image analyzer of particle size and shape. The equipment consists of some devices such as the hopper to carry out the feeding of the abrasive and precision lenses to perform the most accurate analysis. The lenses can be of various sizes. The range used for the evaluation of the size of aluminium oxide was from 26 μm to 2.6 mm. This demonstrates that the average size of the alumina particles was between 300-400 μm (Figure 6). In relation to the morphology of the abrasive particles, these have an angular shape with quite pronounced tips (Figure 7). These micrographs were obtained with a SEM model FE JEOL JSM-7600F and an also Energy-Dispersive X-ray analysis (EDS) was employed to obtain the chemical composition of this particular abrasive. Basically, aluminium oxide is composed of oxygen (O) 10.31 Wt. %, fluorine (F) 4.48 Wt. %, aluminium (Al) 22.33 Wt. %, silicon (Si) 3.47 Wt. %, chromium (Cr) 9.63 Wt. %, iron (Fe) 45.11 Wt. % and nickel (Ni) 4.67 Wt. %.

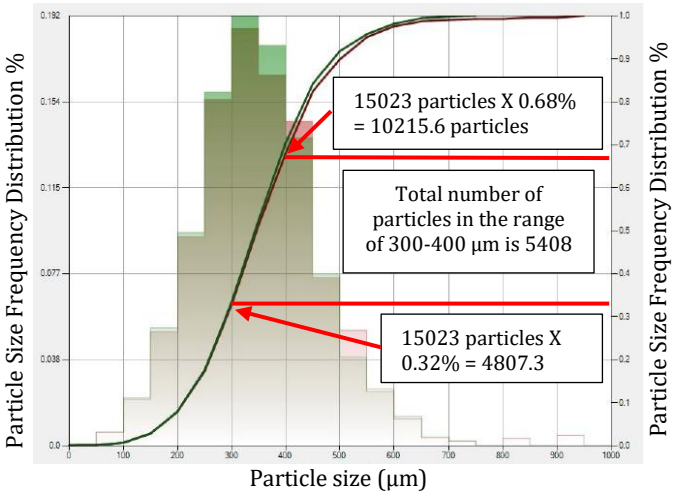

Fig. 6. Particle size distribution.

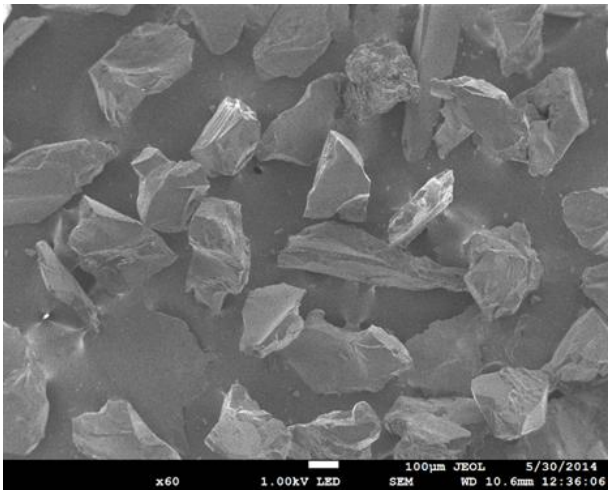

(a)

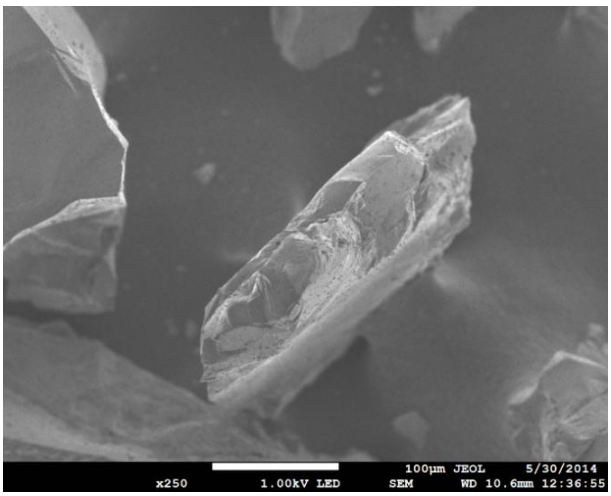

(b)

Fig. 7. Morphology of alumina particles.

2.4 Testing method

An erosion equipment based on ASTM G76 standard [10], was used to perform the tests. The alumina particles impacted the tepetate

ceramic surfaces during 2 min at 30° and 3 min at 45°, 60° and 90°; however, the mass loss of each sample was measured every 1 min. Two tests were performed for each impact angle, 30°, 45°, 60° and 90°. The particle velocity was 5 ± 1 m/s, and the abrasive flow rate was 12 ± 0.5 g/min. In these particular tests, the impact velocity of the erosive particles was very low to prevent the specimens broke on pieces. The samples were situated 8 ± 1 mm from the nozzle end. The temperature during the tests, was between 35°C-40°C. The mass loss data were obtained by using an analytical balance (± 0.0001 g).

3. RESULTS AND DISCUSSION

3.1 Wear scars

Figure 8 presents the wear scar dimensions on tepetate-based ceramic specimens produced by the impact of alumina particles. Here, it is possible to observe that all the samples suffered large and deep craters, after the erosion tests. The wear scars are located in the highest area of the samples at 30° and 45°, whereas the scars are found almost in the central zone at 60° and 90°. The wear scar sizes are larger at 30° and 90°, and even at 90°, a wider wear scar can be observed. At both impact angles, particles can make contact more than once on the surfaces, so the wear scars can be more pronounced at these incident angles.

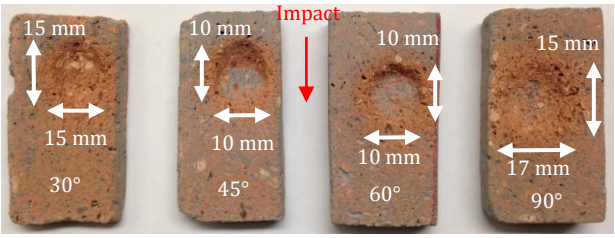

Fig. 8. Wear scars on tepetate-based ceramic specimens.

3.2 Volume loss and Total erosion rates

The results of the mass loss of the tepetate-based ceramic at each impact angle were obtained using the following formula:

$$\text{Mass loss (g)} = \text{Initial weight} - \text{Weight lost every 1 min} \quad (1)$$

It was necessary to obtain an initial weight for each specimen before being eroded. Subsequently, the specimens were removed every 1 min, to measure the mass loss. A digital scale with a capacity to weigh 120 g (model WH Series–Electronic Analytical Balance) was used to perform the weighing measurements. The next step was to determine the volume loss at each impact angle; the formula used was the following. In this particular case, the density of tepetate was employed, 1.9 g/cm^3.

$$\text{Volume loss (mm}^3\text{)} = \text{Mass loss} / \text{Density of test material} \quad (2)$$

Table 1 presents the average volume loss results from the tepetate samples at each impact angle used to perform the erosion tests. It is important to mention that two tests were conducted for each impact angle, for this reason, standard deviations are included. Figure 9 presents the graph of volume loss versus time. A higher mass loss is clearly observed over time for all incidence angles. In this particular case, the closest results were obtained at 45° and 90°, while at 30°, a higher wear rate is observed even without complying with the same time as the tests at the other incidence angles (2 min). The testing time at 45°, 60° and 90°, 3 min, on the tepetate-based ceramic material was very short compared to other materials because this material is highly brittle. The lowest erosion rate, and consequently the angle where this material showed the greatest wear resistance, was 60°. In all cases, the increasing trend in mass loss and therefore volume loss was constant.

Table 1. Average volume loss.

Time (min)	Impact angles			
	30°	45°	60°	90°
1	311.32 ± 1.55	203.84 ± 0.19	176.37 ± 0.09	195.89 ± 1.55
2	638.16 ± 0.9	381.37 ± 0.73	277.05 ± 1.44	354.68 ± 1.65
3	-	464.05 ± 1.31	306.42 ± 0.97	384.16 ± 1.71

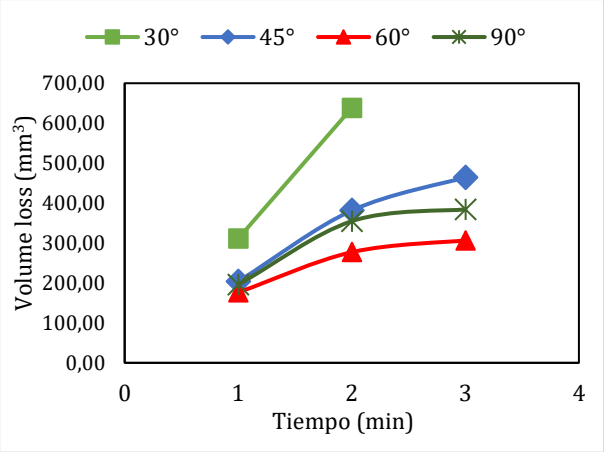

Fig. 9. Graph of volume loss vs time of tepetate samples.

In respect to the total erosion rate (mm3/g), it was obtained by dividing the total volume loss by the total mass of alumina particles, impacting the surface after 3 min at 45°, 60° and 90°, and 2 min at 30°, as indicated in ASTM G76 standard.

$$\text{Total erosion rate } (mm^3/g) = \text{Total volume loss}/\text{Total mass of alumina particles} \quad (3)$$

In this particular case, the total particle mass was obtained using the calculated abrasive flow rate. Therefore, the 12 g was multiplied by 3 min to obtain the total mass of particles impacting the ceramic surface. Thus, the total mass was 36 g for 3 min, and in the case of the sample worn at 30°, the total mass was 24 g in just 2 min, which correspond to the test duration. Table 2, presents the results of the total erosion rate (mm^3/g) at each impact angle. Figure 10 shows the graph of the total erosion rate (mm^3/gr) against the impact angle. As previously mentioned, the highest erosion rate occurred at 30° and was considerably reduced at 60°. Due to this, it is possible to conclude that this tepetate-based ceramic has a ductile behaviour, based on the graph shown in the erosion literature [11]. These results correlate well with the images of the wear scars shown in Figure 8, where it is possible to observe that the damage at 30° is more pronounced and deeper than that observed at the other incidence angles. Of course, the erosion at 45° and 90° is also worth mentioning, since it is possible to see very deep erosion scars.

Table 2. Total erosion rates.

Impact angle (α)	Total Erosion rate (mm^3/gr)
30°	2.66E+01
45°	1.29E+01
60°	8.51E+00
90°	1.07E+01

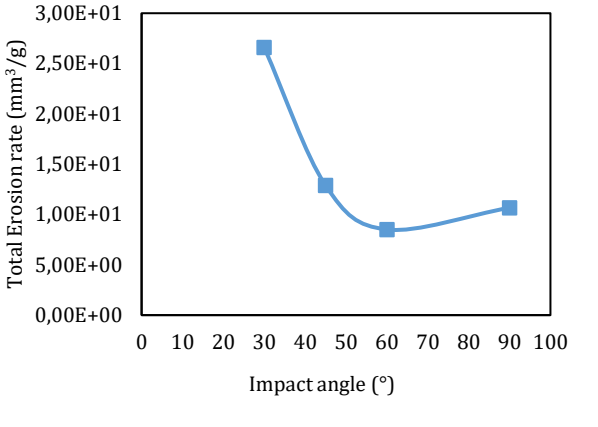

Fig. 10. Graph of total erosion rates vs impact angles.

4. CONCLUSION

The results allow the following conclusions,

1. The abrasive particle had an outstanding performance since the ceramic material was highly damaged, especially at 30°, where the test had to be completed before the other impact angles. This due to the high damage that originated on the material surface.
2. In relation to the erosion rates, the quantitative analysis allowed to confirm that the specimens subject to particle impacts at 30°, presented the greatest volume loss, while a considerable reduction was seen when the incidence angle was 60 °.
3. The ceramic material made from tepetate, although it is a highly fragile material due to its porous nature, in this specific erosion tests, presented a ductile type behaviour, since it reached its maximum erosion rate at 30°. This could be related to the impact and sliding of angular alumina particles, which could cause the removal of a large amount of material, once they made contact with the tepetate specimens.

Acknowledgement

We recognize the experimental support of the Mechanics Laboratory of the Faculty of Mechanical and Electrical Engineering and the Chemical Laboratory of the Faculty of Chemical Sciences from the Universidad Veracruzana in Poza Rica, to complete the present work.

REFERENCES

[1] Material Rústico, *Sillar de Tepetate en Block*. [Online]. Available: https://materialrustico.com/sillar/. Accessed: Oct. 31, 2025.

[2] V. Bonu and H. S. Barshilia, "High-temperature solid particle erosion of aerospace components: Its mitigation using advanced nanostructured coating technologies," *Coatings*, vol. 12, no. 12, pp. 1776–1792, Dec. 2022, doi: 10.3390/coatings12121979.

[3] M. J. Presby, J. L. Stokes, and B. J. Harder, "Solid particle erosion in ceramic matrix composites and environmental barrier coatings: A perspective," *J. Am. Ceram. Soc.*, vol. 107, no. 3, pp. 1776–1792, Mar. 2024, doi: 10.1111/jace.19376.

[4] L. Fengjiao, F. Minghao, L. Yan-gai, and H. Zhaohui, "Solid particle erosion behavior of NiCr–Al_2O_3–ZrO_2 (8Y) ceramic composites," *Key Eng. Mater.*, vols. 512–515, pp. 451–454, Jun. 2012, doi: 10.4028/www.scientific.net/KEM.512-515.451.

[5] G. Portu *et al.*, "Solid particle erosion behavior of laminated ceramic structures," *Wear*, vols. 442–443, p. 203147, Feb. 2020, doi: 10.1016/j.wear.2019.203147.

[6] J. E. Ritter, "Particle impact damage of engineering ceramics," in *Fracture Mechanics of Ceramics*, R. C. Bradt, D. P. H. Hasselman, D. Munz, M. Sakai, and V. Y. Shevchenko, Eds. Boston, MA: Springer, 1992, pp. 555–578.

[7] X. Li *et al.*, "Solid particle erosion–wear behavior of SiC–Si_3N_4 composite ceramic at elevated temperature," *Ceram. Int.*, vol. 40, no. 10, pp. 16201–16207, Dec. 2014, doi: 10.1016/j.ceramint.2014.07.055.

[8] Y. I. Oka, S. Mihara, and T. Yoshida, "Impact-angle dependence and estimation of erosion damage to ceramic materials caused by solid particle impact," *Wear*, vol. 267, nos. 1–4, pp. 129–135, Jun. 2009, doi: 10.1016/j.wear.2008.12.091.

[9] C. A. Cabrera-García, "Elaboración de ladrillo común a base de mezclas de arena, ceniza, barro y tepetate," Bachelor thesis, Facultad de Ciencias Químicas, Universidad Veracruzana, Poza Rica–Tuxpan, 2014.

[10] ASTM G76-95, *Standard Practice for Conducting Erosion Tests by Solid Particle Impingement Using Gas Jets*. West Conshohocken, PA: ASTM International, 2018.

[11] I. M. Hutchings, *Tribology: Friction and Wear of Engineering Materials*. London, U.K.: Edward Arnold, 1992.